Associative Amplitude Modulation with Built-In Noise Immunity

Ron Spencer, Huseyin Dinc and Taner Sumesaglam

Texas A&M University
Electrical Engineering Department
College Station, Texas 77843-3128

ABSTRACT- Single-pattern real-valued spectral associative memories (SAMs) are proposed for coding and recalling sampled analog or multi-valued data patterns over noisy channels. SAMs are frequency-domain formulations of associative memory that combine the extrinsic redundancy of neural networks with the in-phase and quadrature modulation schemes of telecommunications. Data patterns, or "codewords", are encoded into an attractor wave by associative amplitude modulation (AAM), which may be recalled by recurrent associative amplitude demodulation (AAD). Because no attractors are actually stored in the decoder, single patterns may be transmitted, one at a time over a noisy channel with spurious-free recall. Long-range connectivity is made virtually in the frequency domain, allowing both encoder and decoder to scale linearly with pattern dimension. In-phase and quadrature coding schemes are presented with band structures and anti-aliasing constraints for auto- and heteroassociative memory formation and recall. Simulation results are provided that show the accuracy of recall for various Butterworth and Chebyshev filters.

1. INTRODUCTION

Spectral associative memories (SAMs) were introduced in [1]-[4] for transmitting analog and digital data patterns over noisy channels with built-in noise immunity. SAMs are frequency-domain formulations of associative memory that combine the extrinsic redundancy of neural networks with the in-phase and quadrature modulation schemes of telecommunications. Unlike conventional associative memories, which are stored as long-term non-volatile attractors in a weight matrix that specifies short and long-range connectivity, spectral memories are manifested as *attractor waves*, which set up temporary basins of attraction in a spectral decoder that disappear when transmission of the attractor wave ceases. Data patterns, or "codewords", are encoded into an attractor wave by associative amplitude modulation (AAM) and recalled by recurrent associative amplitude demodulation (AAD). AAM disperses the data pattern across the frequency domain, creating extrinsic redundancy, and AAD re-focuses the pattern in the frequency domain for subsequent expansion back into the spatial domain. Long-range connectivity is made virtually by spectral convolution, allowing both encoder and decoder to scale linearly with pattern dimension, or number of data channels to be transmitted in parallel. The price is bandwidth, which scales quadratically or polynomially with pattern dimension. Autoassociative SAMs create the most extrinsic redundancy and highest noise immunity, followed by heteroassociative SAMs, which allow virtual partitioning [2].

Multi-pattern real-valued (analog) SAMs were introduced in [4], where content-addressability was possible; i.e. *which* data pattern was recalled was influenced by initial conditions at the decoder. *However, when the objective is to get information from point A to point B without corruption, rather than content-addressability, single patterns may be transmitted one at a time over a noisy channel, and the initial conditions of the decoder have no bearing on which fixed-point attractor is selected.* In fact, only one fixed-point attractor exists at a time anyway for single-patterns. This is the topic of this paper; i.e. the practical application of real-valued SAMs as multi-channel, multi-carrier modulator/demodulators (modems) for transmitting single patterns.

Two coding schemes are presented in section 2: *In-phase* (I) and *quadrature* (I/Q) coding, which are distinguished by the corresponding attractor wave, i.e. double-sideband (DSB) for in-phase, and single-sideband (SSB) for quadrature, the latter having more relaxed anti-aliasing constraints. Single-pattern heteroassociative recall is also given in section 2. Band structures and anti-aliasing constraints are given in section 3 and the effects of various Butterworth and Chebyshev recall filters are given in section 4. Conclusions are given in section 5.

2. CODING AND RECALL

Like the bipolar SAMs, two association types are possible for single-pattern real-valued SAMs: auto-associative (a single pattern vector $\mathbf{x}$) or heteroassociative (a single pattern vector pair $\mathbf{x}_1,\mathbf{x}_2$). While the autoassociative case offers the most redundancy, thus the most noise immunity, the heteroassociative case offers flexible control over the degree of redundancy and bandwidth requirements. In this paper the autoassociative memory is considered to be a special case of the

0-7803-7057-0/01/$10.00 ©2001 IEEE.

heteroassociative memory since the pattern pair ($\mathbf{x}_1$,$\mathbf{x}_2$) may be two separate patterns or a partitioning of the same larger pattern, but the memory wave is always generated from two coding waves, $s_1(t)$ and $s_2(t)$.[1] When $\mathbf{x}_1=\mathbf{x}_2=\mathbf{x}$, the heteroassociative case reduces to the autoassociative case, hence, the heteroassociative formulation is presented here.

When only one data pattern is encoded at a time (in a single encode/decode period), simplifications in the formulation given in [4] may be made. For multi-pattern real-valued SAMs, the reference wave was scaled by a continuously adapted value in the decoder, which converged to the eigenvalue of one of the encoded data patterns (eigenvectors). The question of *which* eigenvalue (corresponding to which pattern) had to be decided in the decoder so that local information could influence recall (content-addressability). However, when only one data pattern is encoded at a time, only one eigenvalue is needed, hence, the attractor wave may be generated in the encoder and the eigenvalue adaptation circuitry in the decoder may be eliminated.

Spectral coding may be divided into four parts: 1) pattern preparation, 2) synthesis, 3) spectral convolution and 4) attractor wave generation. There are three coding alternatives: 1) in-phase, 2) quadrature, and 3) complex; however, only the first two are presented here in the interest of brevity.

2.1. In-Phase Coding

In-phase coding is the simplest, but produces an upper sideband (USB), as well as a lower-sideband (LSB) in the memory wave. Since only the LSB is used for decoding, part of the signal power is lost. An in-phase spectral encoder is illustrated in Fig. 1.

2.1.1. Pattern Preparation. Each pattern vector must be augmented with two ancillary channels: 1) a fixed reference for preserving unaugmented pattern magnitude and 2) a filler for normalizing augmented pattern magnitude. The reference channel is for regulating the pattern magnitude in the decoder, and the filler channel is used for normalizing pattern magnitude without changing the original data.

Both patterns are augmented such that $N \rightarrow N + 2$, and the value of the filler channel is given by

$$x_{l,N-1} = \sqrt{R^2 - {x_{l,N-2}}^2 - \sum_{i=0}^{N-3} {x_{l,i}}^2} \; ; \; l=1,2 \qquad (1)$$

where l indexes the neural layer (or pattern in the association pair), $x_{l,N-2}$ is the reference channel for preserving pattern intensity, $x_{l,i}$ are the elements of the original data pattern for i=0,1…N-3, and R is the constant magnitude, which must be greater than the magnitude of the longest augmented vector before normalization. If one pattern is shorter than the other, it is padded with zeros to match the dimensionality of the other pattern such that N = max(N_1,N_2).

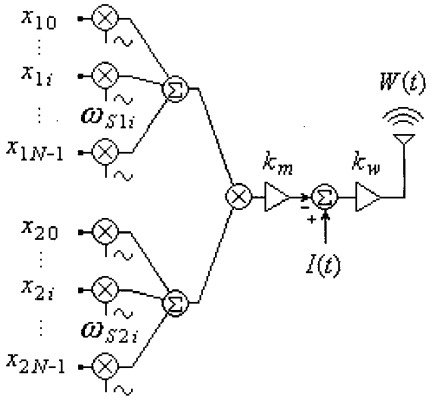

Fig. 1. Block diagram of an in-phase heteroassociative amplitude modulator, or spectral encoder. The autoassociative encoder is architecturally the same, but receives the same data pattern for both sets of local oscillators (LOs).

2.1.2. Synthesis. In-phase coding waveforms, $s_{I1}(t)$ and $s_{I2}(t)$, are defined as the sum of N waveforms, each carrying a sampled analog or ancillary data channel in the amplitude:

$$s_{I1(2)}(t) = \frac{1}{R} \sum_{i=0}^{N-1} x_{1(2)_i} \cos(\omega_{S1(2)i} t) \qquad (2)$$

where $\omega_{S1(2)i}$ are the i^{th} elements of the nonoverlapping carrier frequency vectors $\boldsymbol{\omega}_{\mathbf{S1(2)}}$, defined later.

2.1.3. Spectral Convolution. The memory wave, $M(t)$, which contains extrinsic information about the encoded data pattern, is formed by spectral convolution:

$$M(t) = k_m s_{I1}(t) s_{I2}(t) \qquad (3)$$

where k_m=2 for in-phase coding. Tensor product information is generated in two side bands: a lower-sideband (LSB) and upper-sideband (USB), but only the LSB is used for recall.

2.1.4. Attractor Wave Generation. The attractor wave, $W(t)$, is formed by subtracting the memory wave from a reference wave $I(t)$ which contains energy at diagonal frequencies:

[1] This is opposite to conventional wisdom which holds that the heteroassociative memory is a special case of the autoassociative memory.

$$W(t) = k_w\big(I(t) - M(t)\big) \tag{4}$$

where k_w is a scaling factor for normalizing signal power. Subtracting $M(t)$ from $I(t)$ transfers the encoded patterns from the implied range space into the implied kernel by adjusting the power at diagonal frequencies. This process should not be confused with the subtraction of an identity wave in the bipolar SAM which modifies the implied range space. The DSB identity wave is given by

$$I(t) = \cos(\theta)\sum_{i=0}^{N-1}\cos(\omega_{ILi}t) + \cos(\omega_{IUi}t) \tag{5}$$

where ω_{IL} is the LSB identity frequency vector and $\cos(\theta)$ is the degree of similarity between patterns:

$$\cos(\theta) = \frac{\mathbf{x_1}^T\mathbf{x_2}}{|\mathbf{x_1}||\mathbf{x_2}|}. \tag{6}$$

Average signal power P_s may be normalized by

$$k_w = \sqrt{\frac{P_s}{(N-2)\cos^2(\theta)+1}}, \tag{7}$$

In the autoassociative case $\cos(\theta)=1$, $k_i=1$, and $k_w = \sqrt{P_s/(N-1)}$.

2.2. Quadrature Coding

Quadrature coding is an alternative to in-phase coding which cancels the USB of the attractor wave, increasing the effective signal-to-noise ratio (SNR) for the same power consumption and relaxing the anti-aliasing constraints. The same decoder may be used with potentially different frequencies due to relaxed constraints. The attractor wave is formed as in (4) where

$$M(t) = k_m\big(s_{I1}(t)s_{I2}(t) + s_{Q1}(t)s_{Q2}(t)\big) \tag{8}$$

where k_m=1 and the quadrature waveforms are

$$s_{Q1(2)}(t) = \frac{1}{R}\sum_{i=0}^{N-1} x_{1(2)i}\sin(\omega_{S1(2)i}t) \tag{9}$$

The SSB identity wave is defined by

$$I(t) = \cos(\theta)\sum_{i=0}^{N-1}\cos(\omega_{ILi}t) \tag{10}$$

and the signal power is normalized by

$$k_w = \sqrt{\frac{2P_s}{(N-2)\cos^2(\theta)+1}}. \tag{11}$$

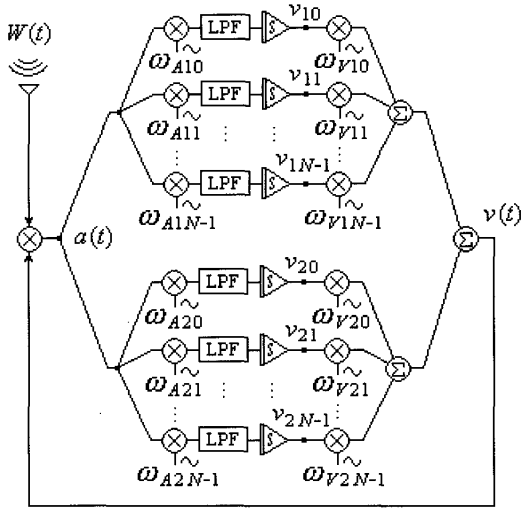

Fig. 2. Block diagram of an in-phase heteroassociative amplitude demodulator, or spectral decoder, which receives SSB (or DSB) attractor waves generated by a quadrature (or in-phase) spectral encoder.

2.3. Spectral Recall

Spectral recall is achieved by recurrent associative amplitude demodulation in which spectral convolution generates inner product information in the frequency domain [1]-[5]. The attractor wave sets up a virtual recall potential with a basin of attraction that corresponds to the encoded pattern. A state wave is continuously refined and spectrally convolved with the attractor wave to compute two linear transformations in which the encoded memory patterns are the kernels. Extrinsic information distributed over the entire attractor band is re-focused into the LSB of the activation wave, which carries the spectral gradient for adaptation. White noise is filtered out over time as the attractor wave provides the only coherent motive.

Spectral recall is divided into four simultaneous parts: 1) synthesis, 2) spectral convolution, 3) analysis, or down conversion and 4) state update. See Fig. 2.

2.3.1. Synthesis. The state wave $v(t)$, is a weighted-sum of individual channel waves across two state bands, one for each pattern in the association:

$$v(t) = \sum_{l=1}^{2}\sum_{i=0}^{N-1} v_{li}\cos(\omega_{vli}t) \tag{12}$$

where $\omega_{v1(2)i}$ are the state synthesis frequencies for the first (second) state vectors, $\mathbf{v}_{1(2)}$. Initially random guesses, $\mathbf{v}_{1(2)}$ converge to scaled versions of the encoded data patterns.

2.3.2. Spectral Convolution. The state wave is spectrally convolved with the attractor wave to produce the activation wave, $a(t)$, into which the spectral gradient is focused:

$$a(t) = v(t)W(t)\,. \tag{13}$$

2.3.3. Analysis, or Down Conversion. The gradient may be extracted by direct conversion at precise analysis frequencies, which requires low-pass filtering (LPF):

$$\frac{\mathrm{d}\mathbf{v}_{\mathbf{1(2)}}}{\mathrm{d}t} = -\mathrm{LPF}(a(t)\cos(\boldsymbol{\omega}_{\mathbf{A1(2)}}t)) \tag{14}$$

where $\boldsymbol{\omega}_{\mathbf{A1(2)}}$ are the analysis frequency vectors of the first (second) recalled patterns. $\mathrm{d}\mathbf{v}_{\mathbf{1(2)}}/\mathrm{d}t$ are the result of linear transformations in which $\mathbf{x}_{\mathbf{1(2)}}$ are the kernels. Taken together, they make up the spatial gradient.

2.3.4. State Update. Recall follows a continuous trajectory which requires integration of the gradient:

$$\mathbf{v}_l = \int \dot{\mathbf{v}}_l \, dt\,; \quad l=1,2. \tag{15}$$

3. BAND STRUCTURES AND ANTI-ALIASING CONSTRAINTS

Carrier frequencies must be separated by integer multiples of $\Delta\omega$, the *beat frequency* and all bands must facilitate tensor product computation in the frequency domain [1]-[4]. $\Delta\omega$ influences both noise immunity and speed of recall; i.e. the higher $\Delta\omega$, the wider the spectrum, the higher the noise immunity, and the greater the allowable speed of recall. Furthermore, all frequency vectors must satisfy anti-aliasing constraints for both coding and recall.

3.1. Band Structures

One set of *coding bands*, which may be used for either autoassociative or heteroassociative coding, is given by

$$\begin{aligned} \omega_{S1i} &= \omega_{S1.L} + Ni\Delta\omega \\ \omega_{S2i} &= \omega_{S2.L} + i\Delta\omega\,, \end{aligned} \tag{16}$$

where $\omega_{S1.L}$ and $\omega_{S2.L}$ are defined later, the index[2] is given by i=0,1,...N-1, and both bands are ascending. (The first band is in *ascending column form* and the second in *ascending row form*.) The diagonal frequency vectors are calculated by

$$\boldsymbol{\omega}_{\mathbf{IL}} = \boldsymbol{\omega}_{\mathbf{S1}} - \boldsymbol{\omega}_{\mathbf{S2}} \quad \text{and} \quad \boldsymbol{\omega}_{\mathbf{IU}} = \boldsymbol{\omega}_{\mathbf{S1}} + \boldsymbol{\omega}_{\mathbf{S2}}\,, \tag{17}$$

[2] In reference [4], i was shown going from 1 to N, but should have been from 0 to N-1, as given in this paper.

where $\boldsymbol{\omega}_{\mathbf{IL}}$ is needed for quadrature coding and both $\boldsymbol{\omega}_{\mathbf{IL}}$ and $\boldsymbol{\omega}_{\mathbf{IU}}$ are needed for in-phase coding.

In the heteroassociative case, *two non-overlapping state bands* are given by

$$\begin{aligned} \omega_{V1i} &= \omega_{V1.L} + Ni\Delta\omega \\ \omega_{V2i} &= \omega_{V2.H} - i\Delta\omega \end{aligned} \tag{18}$$

where ω_{V1i} are the elements of the recalled first data pattern, given in *ascending column form*, and ω_{V2i} are the elements of the recalled second data pattern, given in *descending row form*. The highest and lowest frequencies of the respective bands are given by

$$\begin{aligned} \omega_{V1.L} &= \omega_{V2.H} + B_{V.GAP}\,; \\ \omega_{V2.H} &= B_{S.GAP} + B_{S1} + 2B_{S2} + \Delta\omega \end{aligned} \tag{19}$$

where $B_{S.GAP}$ and $B_{V.GAP}$ are the coding and decoding band gaps respectively [4], and

$$B_{S1} = N(N-1)\Delta\omega \quad \text{and} \quad B_{S2} = (N-1)\Delta\omega \tag{20}$$

are the bandwidths of the respective coding waveforms. Given these definitions, the first state band ends up higher than the second. Finally, the analysis frequencies may be calculated from the synthesis frequencies as follows:

$$\boldsymbol{\omega}_{\mathbf{A1}} = \boldsymbol{\omega}_{\mathbf{V2}} - \boldsymbol{\omega}_{\mathbf{IL}} \quad \text{and} \quad \boldsymbol{\omega}_{\mathbf{A2}} = \boldsymbol{\omega}_{\mathbf{V1}} - \boldsymbol{\omega}_{\mathbf{IL}}\,. \tag{21}$$

For autoassociative recall, only one state band is necessary since $\mathbf{Wv}=\mathbf{W}^{\mathbf{T}}\mathbf{v}$, and it is typically placed one $\Delta\omega$ higher than the LSB of the attractor wave in descending row form (ω_{Vi} in the autoassociative case equals ω_{V2i} in the heteroassociative case). Then the analysis frequencies may be calculated from the synthesis frequencies as follows:

$$\boldsymbol{\omega}_{\mathbf{A}} = \boldsymbol{\omega}_{\mathbf{V}} - \boldsymbol{\omega}_{\mathbf{IL}}\,. \tag{22}$$

3.2. Anti-Aliasing Constraints

Anti-aliasing constraints are provided below for in-phase coding, the worst case. They also work for a SSB attractor wave too; however, they would not be the most relaxed constraints possible.

3.2.1. Heteroassociative. Three anti-aliasing constraints must be satisfied to make the heteroassociative formulation work. First, lower bounds must be placed on the lowest coding frequency to prevent sideband aliasing by the USB of the attractor wave. Second, the width of the coding band gap $B_{S.GAP}$ must be wide enough to allow for alias-free mixing in the decoder. Third, the decoding band gap, $B_{V.GAP}=B_{S1}+\Delta\omega$, must be wide enough to avoid interlayer aliasing. The coding band gap would be calculated by $B_{S.GAP}$ =

ceil($(B_{S2}+ B_{V.GAP}+\Delta\omega)/2\Delta\omega)\Delta\omega$, where ceil(·) rounds up to the next integer, and $\omega_{S2.L}$ = ceil($(3/2)(B_{S1}+B_{S2}+\Delta\omega)/\Delta\omega + B_{V.GAP}/\Delta\omega)\Delta\omega$.

Consider a 2-D example, which could be a balanced partitioning of a 4-D pattern. Both the minimum coding and decoding band gaps would be $3\Delta\omega$. The first and second coding bands would start at $13\Delta\omega$ and $9\Delta\omega$, respectively. In this case,

$$\begin{aligned} \boldsymbol{\omega}_{\mathbf{S1}} &= [13 \;\; 15]^T \Delta\omega, \quad \boldsymbol{\omega}_{\mathbf{S2}} = [9 \;\; 10]^T \Delta\omega \\ \boldsymbol{\omega}_{\mathbf{IL}} &= [4 \;\; 5]^T \Delta\omega, \quad \boldsymbol{\omega}_{\mathbf{IU}} = [22 \;\; 25]^T \Delta\omega \\ \boldsymbol{\omega}_{\mathbf{V1}} &= [11 \;\; 13]^T \Delta\omega, \quad \boldsymbol{\omega}_{\mathbf{V2}} = [8 \;\; 7]^T \Delta\omega \\ \boldsymbol{\omega}_{\mathbf{A1}} &= [4 \;\; 2]^T \Delta\omega, \quad \boldsymbol{\omega}_{\mathbf{A2}} = [7 \;\; 8]^T \Delta\omega. \end{aligned} \tag{23}$$

3.2.2. Autoassociative. Autoassociative recall requires only one virtual layer, which relaxes the anti-aliasing constraints due to no chance of interlayer aliasing. The coding band gap and lowest coding frequency may be simplified to $B_{S.GAP}$ = ceil($n/2)\Delta\omega$ and $\omega_{S2.L} = (n^2+1)\Delta\omega$, respectively, which allow the calculation of all other frequency vectors.

Consider a 4-D example (e.g. two data + two ancillary). The second coding band would start at $17\Delta\omega$ and the band gap would be $2\Delta\omega$. In this case, the coding frequency vectors would be

$$\begin{aligned} \boldsymbol{\omega}_{\mathbf{S1}} &= [22 \;\; 26 \;\; 30 \;\; 34]^T \Delta\omega, \\ \boldsymbol{\omega}_{\mathbf{S2}} &= [17 \;\; 18 \;\; 19 \;\; 20]^T \Delta\omega, \\ \boldsymbol{\omega}_{\mathbf{IL}} &= [5 \;\; 8 \;\; 11 \;\; 14]^T \Delta\omega, \\ \boldsymbol{\omega}_{\mathbf{UL}} &= [39 \;\; 44 \;\; 49 \;\; 54]^T \Delta\omega. \end{aligned} \tag{24}$$

Finally, the highest state frequency would be $\omega_{V.H} = B_{S.GAP}+B_{S1}+2B_{S1}+\Delta\omega = 21\Delta\omega$, leading to

$$\begin{aligned} \boldsymbol{\omega}_{\mathbf{V}} &= [21 \;\; 20 \;\; 19 \;\; 18]^T \Delta\omega, \\ \boldsymbol{\omega}_{\mathbf{A}} &= [16 \;\; 12 \;\; 8 \;\; 4]^T \Delta\omega. \end{aligned} \tag{25}$$

4. SIMULATIONS

4.1. 2-D Example

To demonstrate the noise immunity, a 2-D network was simulated in the presence of noise, in which a clean sine wave was encoded, transmitted, and recalled over a noisy channel. Fig. 3a shows what the sine wave would have looked like if sent directly over the noisy channel in 10dB SNR with no coding gain. Fig. 3b shows the corresponding attractor wave for the first sample and Fig. 3c shows the recalled sine wave. Comparing Fig. 3c with Fig. 3a illustrates the built-in noise immunity.

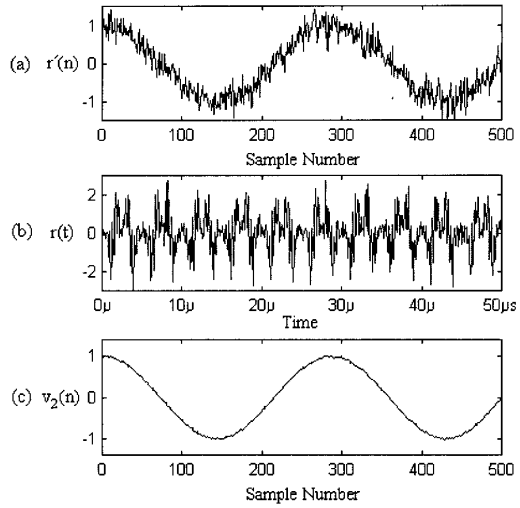

Fig. 3. Transient response of a 2-D autoassociative SAM with a sampled sine wave input: (a) sine wave if sent directly over the noisy channel in 10dB SNR with no coding gain, (b) noisy attractor wave of the first data sample and (c) recalled sine wave. Comparing (c) with (a) illustrates the built-in noise immunity.

4.2. Effect of Higher Order Filters on Recall

Given infinite time for recall, the passbands of the low-pass filters should be as low as possible; however, for faster setting time (faster recall), the bandwidth may be increased as long as the attenuation of beat frequency multiples is not compromised. Thus, without notch filters, the maximum speed of recall is determined by filter order. Using notch filters tuned to integer multiples of the beat frequency allows wider passbands and faster recall.

Several simulations of a 4-D autoassociative network with $\Delta\omega = 2\pi 50$k rad/sec were performed for Butterworth and Chebyshev recall filters of various orders to determine settling time and accuracy of recall. Third, forth, fifth and sixth order recall filters with unity gain passbands were simulated, both with and without notch filters. In each case, the state update integration (15) was absorbed into the definition of the LPF. The settling times and accuracy of recall are given in Tables 1 and 2. For low accuracy, low order filters were generally faster, but for greater accuracy, higher order filters reduced the settling time. Chebyshev filters [6] allowed slightly wider passbands, which led to shorter settling times for fewer bits of accuracy.

For the given band structures and beat frequency, the highest Nyquist frequency for low accuracy recall (1 or 2 bits) was approximately 30kHz/ch using notch filters. For

higher accuracy (5 or 6 bits) the highest Nyquist rate was approximately 6-12kHz/ch.

Inserting a notch filter at $\Delta\omega$ in cascade with the LPF allowed the beginning of the stopband to be doubled, which increased the width of the passband and increased the speed of recall. Whereas the stopband of the LPFs with no accompanying notch filter was forced to start at $\Delta\omega$, the stopband with a notch filter was doubled to $2\Delta\omega$. Several stopband attenuations were simulated: α_{min}=40, 50, and 60dB, which indirectly determined the end of the passband. The settling times for α_{min}=40dB were consistently better, due to the effect on bandwidth. All simulations were performed with ideal macromodels in *Spectre* with R=1 and a reference of .707 volts, where the full range was 0–.707 volts.

5. CONCLUSIONS

Single-pattern real-valued spectral associative memories were presented that allow the coding and recall of analog data patterns over noisy channels by associative amplitude modulation and demodulation. Two coding schemes were presented: in-phase and quadrature for autoassociative and heteroassociative memories. Real-valued SAMs may be thought of as multi-channel, multi-carrier MODEM-CODECs due to the built-in extrinsic redundancy provided at the level of modulation. Autoassociative SAMs provide the most coding redundancy, followed by heteroassociative SAMs. Due to the spectral representation of attractors, long-range connectivity is made virtually in the frequency domain and the physical realization scales linearly.

Simulations show that low order filters are best for low accuracy, while higher order filters are necessary to reduce the settling time for more accurate recall. Notch filters can significantly increase the speed of recall by allowing wider passbands. It remains to be seen how real-valued SAMs will compare with conventional MODEMs in terms of noise immunity and baud rate.

REFERENCES

[1] R. Spencer, "Bipolar spectral associative memories," *IEEE Trans. on Neural Networks*, vol. 12, no. 3, pp. 463-474, May 2001.

[2] R. Spencer, "Nonlinear spectral associative memories: Neural encoders and decoders for digital communications," In: *Intelligent Engineering Systems Through Artificial Neural Networks*, C.Dagli, A. Buczac, J.Ghosh, M.Embrechts, O.Ersoy, and S.Kercel (Eds), ASME Press, vol. 10, pp 971-976, 2000.

[3] R. Spencer, "Nonlinear heteroassociative spectral memories: Virtually partitioned neural encoders and decoders for digital communications," *Proc. of the 2000 ICSC Symposia on Intell. Systems & Applications (ISA 2000)*, F. Naghdy, F. Kurfess, H. Ogata, E. Szczerbicki, H. Bothe, and H. Tlanfield (Eds.), Wollongong, Australia, ICSC Academic Press, Dec, 2000.

[4] R. Spencer, "Multi-pattern real-valued spectral associative memories," *IJCNN 2001*, Washington D.C., July 14-19, 2001.

[5] A. Mondragon, R. Carvajal, J. Pineda de Gyvez, and E. Sanchez-Sinencio, "Frequency domain intrachip communication schemes for CNN," *5th IEEE Int'l Workshop on Cellular Neural Networks & Their Applications*, London, England, Apr., 1998.

[6] R. Schaumann and M.E. Van Valkenburg, *Design of Analog Filters*, Oxford University Press, NY, 2001.

Table 1. Settling times for Butterworth recall filters (B) of various order, with and without notch filter (N) (α_{min}=40dB).

Bits Accuracy	B3 T_s (μs)	B4 T_s (μs)	B5 T_s (μs)	B6 T_s (μs)
1	30	27	27	27
2	30	58	55	55
3	85	66	78	78
4	123	96	90	83
5	142	123	112	107
6	Inf	Inf	163	147
Bits Accuracy	B3 + N T_s (μs)	B4 + N T_s (μs)	B5 + N T_s (μs)	B6 + N T_s (μs)
1	19	18	17	17
2	20	18	17	17
3	50	42	38	37
4	55	45	41	42
5	80	64	55	43
6	Inf	93	Inf	81

Table 2. Settling times for Chebyshev recall filters (C) of various order, with and without notch filter (N) (α_{min}=40dB).

Bits Accuracy	C3 T_s (μs)	C4 T_s (μs)	C5 T_s (μs)	C6 T_s (μs)
1	26	21	24	24
2	27	54	67	53
3	94	112	75	105
4	155	Inf	128	157
5	Inf	Inf	148	Inf
6	Inf	Inf	Inf	Inf
Bits Accuracy	C3 + N T_s (μs)	C4 + N T_s (μs)	C5 + N T_s (μs)	C6 + N T_s (μs)
1	18	14	17	15
2	25	34	17	36
3	52	41	43	45
4	55	64	47	69
5	Inf	89	75	104
6	Inf	Inf	Inf	Inf